Jet Propulsion Laboratory
California Institute of Technology

JPL Document D-93726

TECHNOLOGY DEVELOPMENT FOR EXOPLANET MISSIONS

Technology Milestone Whitepaper

DEMONSTRATION OF STARSHADE STARLIGHT-SUPPRESSION PERFORMANCE IN THE FIELD

Tiffany Glassman, Principal Investigator
Northrop Grumman

Oscar Bruno (Mathematical Systems)

Webster Cash, Anthony Harness (University of Colorado)

N. Jeremy Kasdin, Robert Vanderbei (Princeton)

Suzanne Casement, Steve Warwick (Northrop Grumman)

1 May 2014

National Aeronautics and Space Administration
Jet Propulsion Laboratory
California Institute of Technology
Pasadena, California

1. Objective

In support of NASA's Exoplanet Exploration Program and the Technology Development for Exoplanet Missions (TDEM) component of NASA's Strategic Astrophysics Technology (SAT) solicitation, this whitepaper explains the purpose of the TDEM Milestone for demonstration of starshade starlight-suppression performance in the field, specifies the success criteria against which the milestone will be evaluated, describes the differences between the field implementation and future flight implementation of the starshade, and outlines the milestone demonstration procedure.

2. Milestone Description

Technology milestones serve to gauge the developmental progress of technology for a space-based mission and the mission's readiness to proceed from pre-formulation to formulation. The completion of the milestones described here is to be documented in a report by the Principal Investigator and reviewed by NASA HQ.

The following milestones address broadband starlight suppression using a starshade. This is a scaled-down version of the flight system using a starshade approximately 60 cm in diameter. The milestones will be demonstrated using the already-proven method of testing at long (≥1 km) distances in a field environment (Glassman et al. 2013).

The milestones are stated as follows:

> Milestone #1: Demonstrate, using a starshade, contrast better than 10^{-9}, at all radii past the starshade tips, in 50% bandwidth light.
>
> Milestone #2: Demonstrate agreement between the measured and predicted contrast resulting from a range of starshade shapes.

3. Success Criteria

The following are the required elements of the milestone demonstrations. Each element includes a brief rationale.

3.1. For both Milestones, the contrast is defined as the "contrast image" (i.e. the image with the starshade in place) divided by the peak of the point spread function (PSF) of the unblocked light source. Specific contrast metrics (as in 3.2 and 3.3) can then be measured in this image. The unblocked light source will be imaged at regular intervals close in time to the contrast images. This is expected to be about every 30 minutes, between sets of contrast images. The atmospheric conditions (as determined by the width of the PSF of point sources in each image) will be matched as closely as possible between the contrast image and unblocked source image. Based on previous tests (Glassman et al. 2013) there were periods of atmospheric stability where the size of the PSF was very stable across a set of contrast images and unblocked light source images. If we find that atmospheric conditions are changing rapidly (as determined from the PSF of off-axis sources in the contrast images), then the unblocked light source will be observed more often.

Rationale: Since this field testing is conducted in atmospheric conditions, the seeing of the images can vary widely over the course of a night. In images with better seeing (narrower PSF), the source has a higher peak to total flux ratio and therefore the contrast will appear better. We will use the peak of the PSF as actually measured in the images. Using unblocked source images and contrast images taken close in time and with similar seeing conditions minimizes any differential effects of atmospheric conditions between them. In addition, repeated collection of the same data many times over the course of

the night, and over many nights, allows data with bad or highly-variable seeing conditions to be discarded.

3.2. For Milestone #1, we will measure the contrast achieved as three times the standard deviation (i.e. the 3σ noise level) in the contrast image. This 3σ contrast upper limit represents the faintest point source that could be detected in the image. This contrast upper limit will calculated in an area the size of the PSF of the image at a range of distances from the starshade center, starting at the tips of the starshade petals (see Figure 1). This Milestone will be accomplished using the best starshade we have built and tested by the end of this program.

This analysis is done after subtraction of a smooth background distribution. This background distribution may be a single value for all image positions or may vary smoothly in the radial direction, as expected for dust scattering light from the source. Structures in the image (such as the tripod supporting the starshade, the ground, and off-axis LED light sources) will be also masked out before the contrast is measured.

Rationale: The images in our field tests are background limited, therefore the contrast achieved at image positions past the edge of the starshade is limited by the noise in that background. The background itself (resulting primarily from light scattering from dust in the air) is not relevant to the flight system and is present in a smooth distribution that is easily subtracted. At field positions beyond the petal tips, any stray light from the starshade is expected (based on our modeling) to be at a much lower level than the stray light from the dust scatter. The dust distribution itself is seen to follow the expected fall-off versus radius and this modeled distribution will be used to accurately account for the contribution of the dust.

The petal tips define the inner working angle for a starshade image and there is no outer working angle. Other objects in the field of view contribute stray light but have nothing to do with the starshade performance, so they are not included in the result.

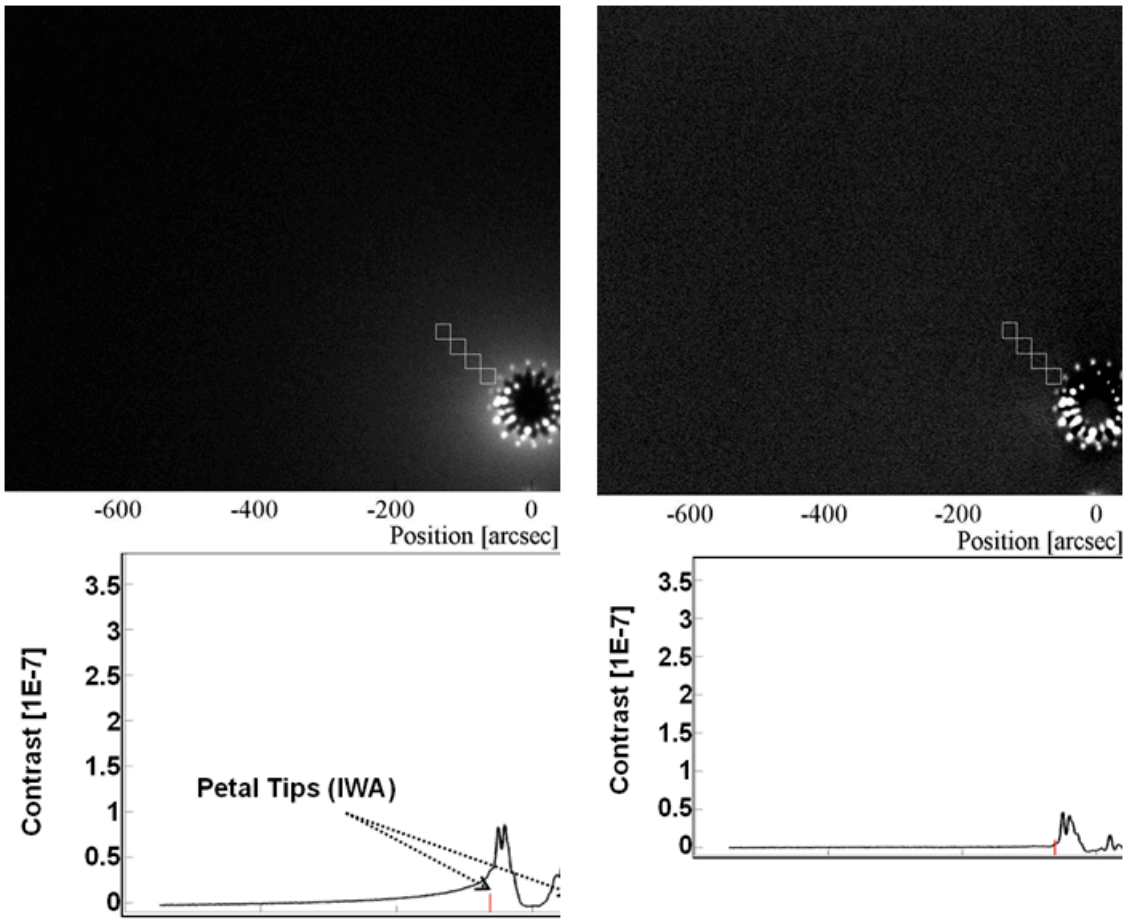

Figure 1: An example of a contrast image that will be taken during this test. On the left is the original contrast image with areas of the field containing other structures (such as the starshade tripod) masked off (Glassman et al. 2013). The white boxes represent regions where the 3σ contrast upper limit is measured. The contrast upper limit achieved in each box was 1.1×10^{-8} (at 75"), 9.6×10^{-9} (at 105"), 9.1×10^{-9} (at 136"), and 8.5×10^{-9} (at 167"). The plot on the bottom is an azimuthal average of the image showing the effect of the dust halo.
On the right, this dust halo has been subtracted and the background is essentially flat. The contrast upper limit achieved in each box in this case was 9.1×10^{-9} (at 75"), 8.9×10^{-9} (at 105"), 8.7×10^{-9} (at 136"), and 8.5×10^{-9} (at 167"). As expected, these results are very similar to the upper limits before background subtraction. Milestone #1 will use the 3σ noise in the white boxes in such an image using the best starshade that we have built by the end of the program. Milestone #2 will compare the brightness of individual point sources caused by flaws in the starshade shape (similar to those seen here due to the petal tips and valleys) to the predicted diffraction from the same flaws.

3.3. For Milestone #2, the contrast predicted from deliberate flaws in the shape of the starshades will be measured by calculating the total flux located at the image position of that flaw. For example, a truncated starshade tip will create a source of light at the location of the tip (see Figure 1). The total amount of light (in contrast units) will be measured within an aperture centered on that location. The predicted brightness of that source will be determined by measuring the dimensions of the starshade flaw, incorporating the as-built flawed shape into our numerical simulation of starshade diffraction, and finding the total amount of light (in contrast units) in the same aperture in the simulated image.

Examples of flaws that may be built, tested, and simulated are truncated petal tips and valleys, misplaced petals, and full starshade motions (such as tilting and clocking). We will identify families of shape errors that are representative of the shape errors expected in on-orbit starshade struc-

tures (such as from manufacturing imperfections, thermal distortion, deployed alignment tolerances, and operational stability). Several starshades will be built with these shape errors exaggerated for the purposes of model correlation. The measured and modeled predictions will be compared and the resulting differences will be quantified as an uncertainty to be applied to future predictions of the contrast effect of untested starshade shapes. Note that this work will not predict or allocate the level of such shape flaws that are expected in the on-orbit case; we will only validate that the model can accurately predict the diffraction from such shapes.

Rationale: In order to validate the predictions of our numerical starshade simulation, we must compare the measured performance to predictions from the same starshade shape. A perfect starshade would have no signature that could be closely matched to predictions, especially since any such effect would be hidden by background flux in the test measurement. Since the effect of a flaw in the starshade shape is localized, a comparison of the measured and modeled contrast for individual flaws will provide a method to validate the model.

3.4. For Milestone #1, no wavelength-limiting filters will be used in measuring the contrast for demonstration of the milestone. The wavelength range will be determined by the capabilities of the white-light LED light sources, the telescope optics, the detector, and Neutral Density (ND) filters needed to get the required dynamic range. For Milestone #2, we will also take observations using broadband filters in order to compare the modeled and measured wavelength dependence of the starshade performance.

The wavelength performance of each of these elements will be measured or determined from spec sheets and reported. Specifically, we will include the measured transmission of the ND filters versus wavelength and the measured linearity of the detector. These are the two critical factors in comparing the contrast images to the unblocked star images. The measurement accuracy of these calibration factors will be included in the final reported errors in the measured contrast.

Rationale: No wavelength restrictions are needed for demonstrating starshade performance. Based on data from our earlier tests (Glassman et al. 2013), we expect that the optics will provide a bandwidth of ~50%. The careful calibration of the ND filters and detector linearity is needed because any errors in these factors directly translate to errors in the contrast.

3.5. The contrast measurements (3.2 and 3.3) must be satisfied on three separate occasions with a reset of the starshade alignment between each demonstration.

Rationale: This provides evidence of the repeatability of the contrast demonstration. The reset of the alignment of the starshade and the telescope between data sets ensures that the three data sets can be considered as independent and do not represent an unusually good configuration that cannot be reproduced. There is no required interval between demonstrations; subsequent demonstrations can begin as soon as prior demonstrations have ended.

4. Differences between Laboratory Demonstration and Flight

Environment

The milestone will be achieved in a field environment with an artificial light source rather in a space environment with a star. This leads to a number of differences between test and flight but does not affect the validity of the starlight suppression demonstration.

The outdoor test environment leads to variations in the transmission and blurring of the light source. These effects are mitigated by taking calibration images of the unblocked source close in time to the contrast images.

Dust in the air scatters light from the source into the telescope. This creates a smooth background that is the limiting source of flux at radii larger than the starshade tips. Photon noise from this background is expected to be the largest noise contributor. This will limit our reported best contrast at large angles from the starshade center, though localized effects from the starshade will appear at small angles and will be compared to model predictions (as seen in Figure 1).

Starshade system architecture

The starshade system architecture adopted for these milestones is scaled down from the flight system. The scale of the field test is approximately 1/100th of the flight system design called New Worlds Observer (NWO; Cash et al. 2009) which uses a 62 meter diameter starshade operating 80,000 km from a 4 m telescope. The field test is currently operating at a Fresnel number that is ~20X higher than this flight system. However this is still within the same optical regime and the same numerical simulation is valid over this range (Glassman et al. 2013; Sirbu et al. 2011; Samuele et al. 2010; Schindhelm et al 2007). That is, the same numerical simulation, without any changes, can be used to predict the performance of the full-scale system and the scaled-down system that will be tested here. Therefore the field test serves the purpose of validating the predictions of the simulation, which can then be used to predict the performance of the on-orbit starshade. This test will not define the starshade shape flaws that will contribute to the on-orbit contrast performance or produce an error-budget for such a mission. Instead this test is focused on validating that the contrast performance predicted by the numerical simulation for a small set of well-defined starshade shapes matches what is measured for those shapes.

5. Milestone Validation Procedure

The starshade is removed from the line of sight between the telescope and the light source. The main light source is a 1W, white-light LED focused into a beam 0.4-3° wide. Additional white-light LEDs are placed off-axis from the main light source and reduced in brightness by factors of ~10^5 – 10^9. These sources simulate planets and probe the atmospheric conditions in each image.

Short (~0.1 second) images of the unblocked light source are taken, using ND filters in the camera to ensure we don't saturate the detector.

The starshade is realigned to the line of sight using observations with the telescope and verbal commands to the operator at the starshade location. This typically takes a few minutes.

A series of longer (2-10 second) exposures with no ND filters are taken with the starshade blocking the light source. This series will typically take ½ hour to 1 hour. The series of exposures taken during this time is averaged together later to produce the contrast image. Care is taken that the contrast exposures and unblocked-star images that are later compared were taken under stable atmospheric conditions (see Glassman et al. 2013).

The starshade is removed from the telescope line of sight and the unblocked star is observed again.

For Milestone #1, this procedure is conducted with the best starshade that has been built.

For Milestone #2, this procedure is conducted with starshades with a variety of shapes containing deliberate flaws.

6. Milestone Certification Data Package

The calculation of the contrast metrics will be according to established Program guidelines.

The following data or data images to be presented in a final report:

1. Model predictions of contrast performance for specific as-measured starshade shapes
2. Calibrated images of the unblocked light source
3. A set of contrast images
4. A contrast metric value for the target areas in each of the contrast images (3σ upper limits for Milestone #1 and total flux of localized sources for Milestone #2).

The source data of images will be made available to the Exoplanet Exploration Program.

7. Milestone Report

The Principal Investigator will assemble a milestone report for review by the Exoplanet Exploration Program and its Technology Assessment Committee (TAC). In the event of a consensus determination that the success criteria have been met, the Program will submit the findings of the ExEP TAC to NASA HQ for official certification of milestone compliance. In the event of a disagreement between the Program and the TAC, NASA HQ will determine whether to accept the data package and certify compliance or request additional work.

8. Approvals

Approved/ _____ 6/17/2014

Tiffany Glassman
Principal Investigator, Northrop Grumman

Date

Approved/ _____ 6/23/2014

Peter Lawson
Exoplanet Exploration Program Chief Technologist, JPL

Date

Approved/ _____ 7/1/2014

Gary Blackwood
Exoplanet Exploration Program Manager, JPL

Date

Approved/ _____ 7/29/2014

Douglas Hudgins
Exoplanet Exploration Program Scientist, NASA HQ

Date

Appendix A: State of the Art of Starshade Optical Modeling and Testing

A. 1. Numerical Simulations

The members of this team have developed several high-fidelity numerical codes for modeling the diffraction performance of starshades, using a variety of numerical methods (Cash 2011; Glassman et al. 2010; Dumont et al. 2009). We have performed detailed comparisons between several of these models and found that the results agree to within ~5% (Shaklan et al. 2010). These models are used to predict on-orbit performance of starshade missions and optimize starshade designs. They are also used to predict the effect on the performance of flaws in the shape of the starshade and thus create error budgets for the level of shape errors that can be tolerated. Since the optical performance of the full-scale starshade system cannot be tested from the ground, numerical modeling, validated by sub-scale tests, will be critical to the mission success.

A. 2. Small-Scale Laboratory Testing

Previous sub-scale testing established basic agreement between models and measurements of starshades a few cm in diameter in laboratory testbeds (Samuele et al. 2010; Sirbu et al. 2011; Schindhelm et al 2007). With these testbeds, several key performance metrics in the model have been validated; in particular, the simulated contrast has been matched to within ~50% and the observed structures in the images have been qualitatively matched. Additionally, our sub-scale testing has demonstrated contrast levels of $\sim 10^{-7}$ with the same starshade shape design, F#, and resolution as the flight configuration (Samuele et al. 2010). These efforts brought the performance verification and model validation to TRL 3. However, these small starshades have micron-sized features that may introduce complex and difficult-to-simulate effects because the sizes of the features are close to the observation wavelength. These interactions are not relevant to the full-scale starshade. Other testbeds achieved fainter contrast levels for other configurations that are not direct analogies of the on-orbit system.

A. 3. Field Testing

The state of the art of optical testing of medium-scale starshades has been performed by this team over the past two years. In a series of three tests we showed that the approach is feasible and measured contrast of $\sim 1\text{-}2 \times 10^{-8}$. In each test, we learned more about the limitations, made corrections to the equipment or testing procedures, and improved the results.

This method eliminates issues with collimating optics, manufacturing accuracy, and non-analogous configurations that limited the previous starshade testbeds. It provides a more robust demonstration of the starshade performance than in the tightly-controlled conditions of a lab, demonstrating the adaptability of the starshade design. In fact our completed tests at this scale have shown that we reach the performance limit of the starshade much more rapidly than we did with the tube tests of smaller starshades – less time was spent debugging lab issues that are not relevant to flight.

In the latest field test (Glassman et al. 2013), a bright “star” and off-axis LEDs in the Field of View (FOV), let us select images where the “star” was well aligned behind the starshade and even to sort contrast images by the atmospheric seeing in the individual frame

(

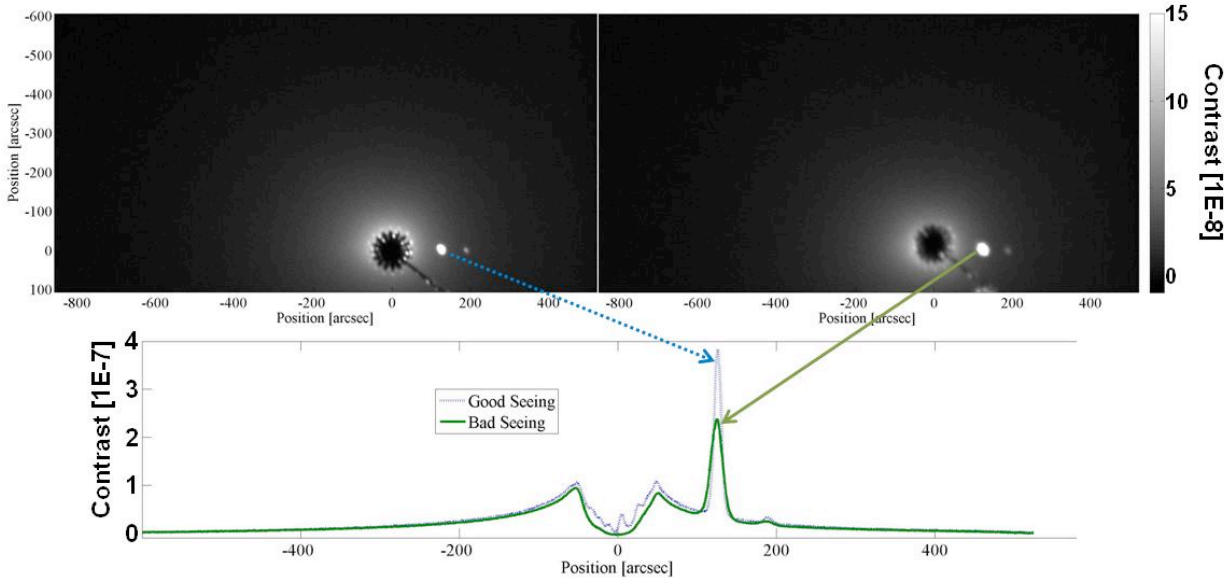

Figure **2**). During this test, we clearly observed the optical impact from the shape of the starshade not quite meeting the ideal. The contrast of these features due to imperfect starshade tips was ~1x10^{-7}. However the factor that limited the contrast in these images was a halo around the starshade caused by forward scattering off dust in the air. The measured contrast at the edge of the starshade (the Inner Working Angle or IWA) was ~1-2x10^{-8}, averaged over a region between the petals. We also measured the performance of a starshade with large, flawed valleys and with flaws added by hand in three locations

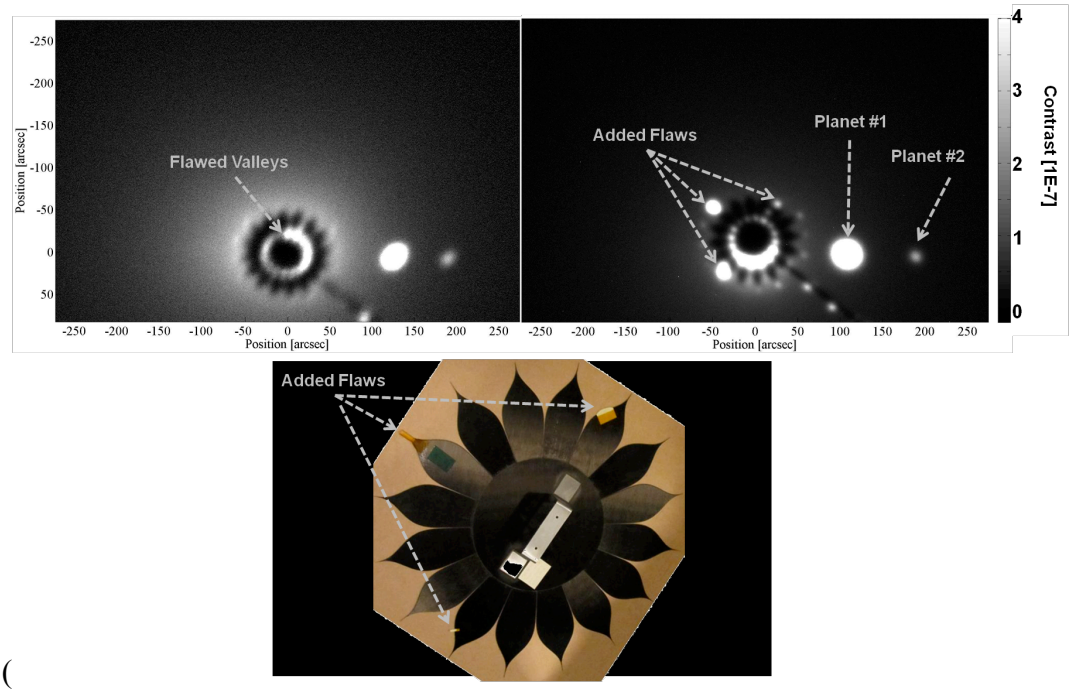

(

Figure **3**) and saw the expected localized effects in the image.

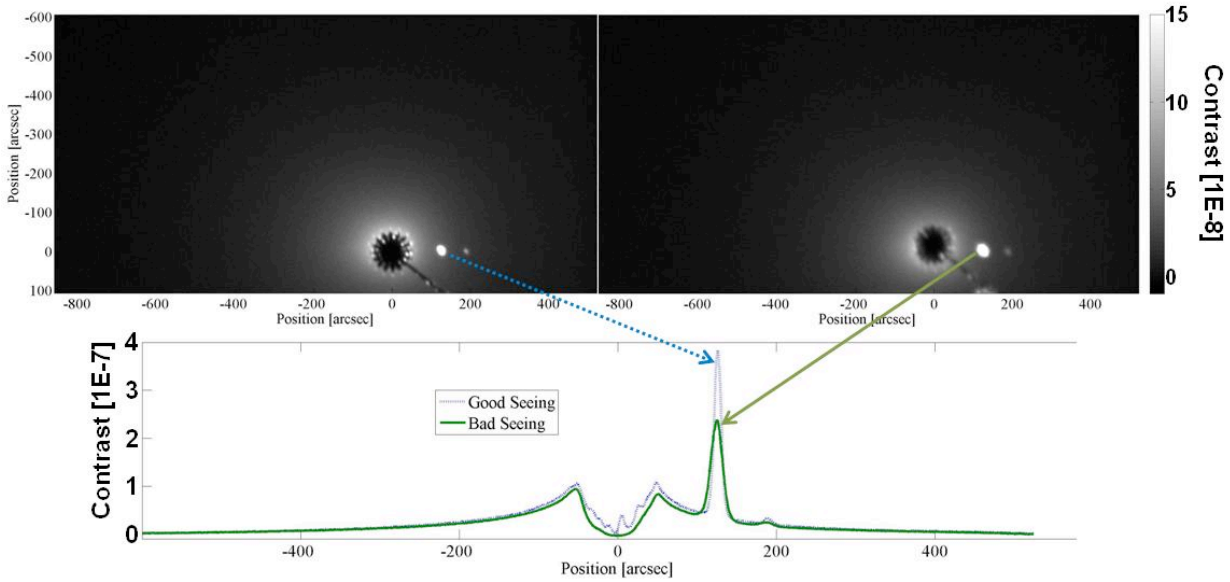

Figure 2: Measured Contrast Images. ***Two data sets of seven images each, one set with good seeing (~7-10") and one set with bad seeing (~15-18"), are compared. Although the artificial planet point sources have wider PSFs, the contrast limit in the image is unchanged. This is true as long as the image motion is less than the IWA of the starshade (60" or 3-8X the resolution).***

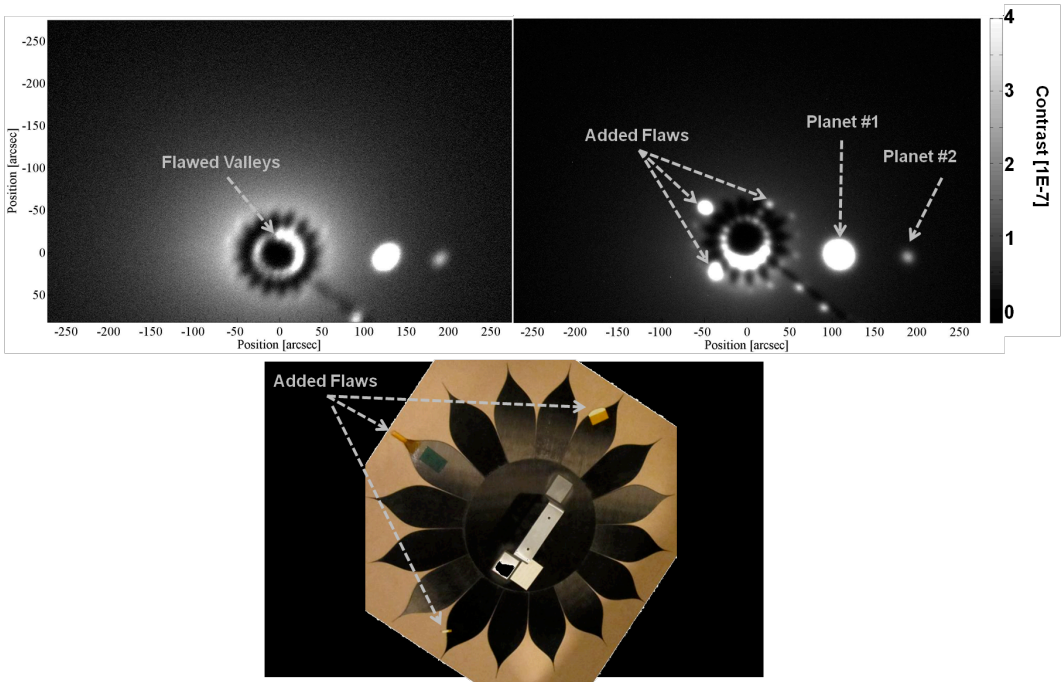

Figure 3. Measured Contrast Due To Added Errors. ***Starshade 3 has valleys that are significantly too wide. These flaws result in bright peaks in the contrast image at the positions of the valleys (top left). In addition, we added extra flaws to this starshade by taping paper to it in three locations (bottom). These additional shape flaws led to additional point sources in the contrast image (top right).***

References/ Bibliography

Casement, L. S., Glassman, T., Lo, A., Warwick, S., Armagan, O., "Field Testing of a 1/100th Scale Starshade," Bulletin of the American Astronomical Society, 221, 305.09 (2013).

Cash, W. "Analytic Modeling of Starshades," Astrophysical Journal, 738, 76 (2011).

Cash, W. "Detection of Earth-like planets around nearby stars using a petal-shaped occulter," Nature, 442, 51 (2006).

Cash, W., et al., "The New Worlds Observer: the Astrophysics Strategic Mission Concept Study," Proc. SPIE, 7436, 5 (2009).

Dumont, P., Shaklan, S., Cady, E., Kasdin, J., and Vanderbei, R., "Analysis of External Occulters in the Presence of Defects," Proc. SPIE, 7440, 6 (2009).

Glassman, T., Casement, S., Warwick, S., Armagan, S., and Donovan, J. "Achieving High Contrast Ratios with a 60 cm Starshade," Proc. SPIE, 8864, 42, (2013).

Glassman, T., Johnson, A., Lo, A., Dailey, D., Shelton, H., and Vogrin, J., "Error Analysis on the NWO Starshade," Proc. SPIE, 7731, 161 (2010).

Kasdin, N. J., Cady, E., Dumont, P., Lisman, P., Shaklan, S., Soummer, R., Spergel, D., and Vanderbei, R., "Occulter Design for THEIA," Proc. SPIE, 7440, 3 (2009).

Kasdin, N. J., Lisman, D., Shaklan, S., Thomson, M., Cady, E., Martin, S., Marchen, L., Vanderbei, R. J., Macintosh, B., Rudd, R. E., Savransky, D., Mikula, J., and Lynch, D., "Technology demonstration of starshade manufacturing for NASA's Exoplanet mission program," Proc. SPIE, 8442, 0A (2012).

Kern, B., Kuhnert, A., & Trauger, J., eds., "Exoplanet Exploration Technology Milestone #2 Report," Jet Propulsion Laboratory Publications, Pasadena, California, JPL Document 60951 (2008).

Lawson, P. R., "Exoplanet Exploration Program Technology Plan Appendix: 2012," Jet Propulsion Laboratory Publications, Pasadena, California, JPL Document D-72279 (2013).

Lo, A., Glassman, T., Dailey, D., Casement, S., and Marks, G., "Technology Development for the Starshade to Enable High Contrast Imaging," IEEE Aerospace Conference, 6187185 (2012).

Mawet, D., et al., "Review of small-angle coronagraphic techniques in the wake of ground-based second-generation adaptive optics systems," Proc. SPIE, 8442, 04 (2013).

NRC Astronomy and Astrophysics Survey Committee, "New Worlds, New Horizons in Astronomy and Astrophysics," The National Academies Press, Washington, DC (2010).

Samuele, R., Varshneya, R., Johnson, T., Johnson, A., and Glassman, T., "Progress at the Starshade Testbed at Northrop Grumman Aerospace Systems – Comparisons with Computer Simulations," Proc. SPIE, 7731, 51 (2010).

Schindhelm, E., Shipley, A., Oakley, P., Leviton, D., Cash, W., and Card, G., "Laboratory Studies of Petal-Shaped Occulters," Proc. SPIE, 6693, 5 (2007).

Shaklan, S., Noecker, C., Glassman, T., Lo, A., Dumont, P., Kasdin, J., Cady, E., Vanderbei, R., and Lawson, P., "Error Budgeting and Tolerancing of Starshades for Exoplanet Detection," Proc. SPIE, 7731, 75 (2010).

Sirbu, D., Cady, E., Kasdin, J., Vanderbei, R., Lu, J., and Kao, E., "Optical Verification of Occulter-Based High Contrast Imaging," Proc. SPIE, 8151, 14 (2011).

Trauger, J., Kern, B., & Kuhnert, A., eds., "TPF-C Technology Milestone #1Report," Jet Propulsion Laboratory Publications, Pasadena, California, JPL Document 35484 (2006).

Turnbull, M., Glassman, T., Roberge, A., Cash, W., Noecker, C., Lo, A., Mason, B., Oakley, P., and Bally, J., "The Search for Habitable Worlds: 1. The Viability of a Starshade Mission," Publications of the Astronomical Society of the Pacific, 124, 418 (2012).

Vanderbei, R., Cady, E., and Kasdin, J., "Optimal Occulter Design for Finding Extrasolar Planets," Astrophysical Journal, 665, 794 (2007).